CO, N_2O, CH_4, and CO_2 have negligible absorption at the visible and NIR wavelengths relevant to ocean color remote sensing. However, O_2, O_3, NO_2, and H_2O have absorption bands in the visible and NIR. The O_2 and H_2O bands can be avoided by judicious choice of sensor bands, as shown in Fig. figure1 for the MODIS bands. However, as seen in Figs. figure2 and figure3, O_3 and NO_2 have broad, concentration-dependent absorption bands that cannot be avoided. It is therefore necessary to account for absorption by these two gases.

The concentrations of absorbing gases are usually measured as column concentrations, i.e., the number of molecules per unit area, or as the equivalent in Dobson units. One Dobson unit refers to a layer of gas that would be $10\,\mu m$ thick at standard temperature and pressure, or about 2.69×10^{16} molecules cm^{-2}. 1000 DU = 1 atm-cm; that is, 1000 DU is the number of molecules that would give a layer of gas 1 cm thick at a pressure of one atmosphere.
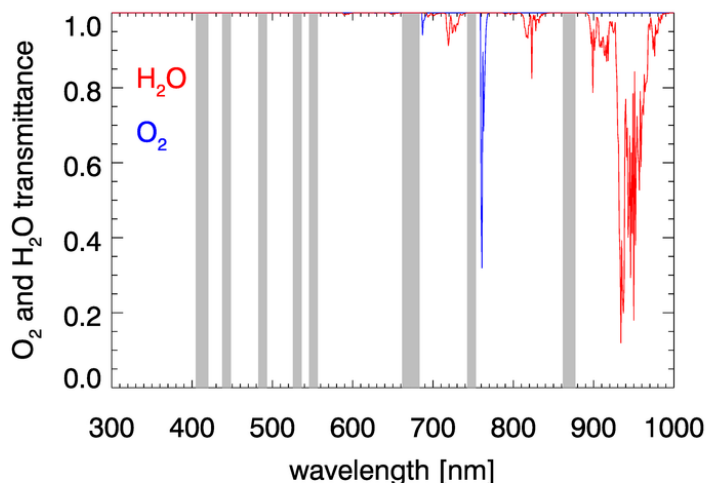

Figure 1: Transmittance by O_2 and H_2O for a moist tropical atmosphere. The resolution is 1 nm. The MODIS sensor bands are shaded in gray.

For optically thin absorbing gases that are high in the atmosphere (O_3 in particular), it is possible to correct for absorption using just the geometric air mass factor M computed by

$$M = \frac{1}{\cos\theta_s} + \frac{1}{\cos\theta_v} \tag{1}$$

because scattering is not significant. However, for gases near the surface (NO_2 in particular), multiple scattering by dense gases and aerosols is significant and increases the optical path length, hence the absorption. Thus M is not a good approximation for the total optical path length through an absorbing gas near sea level.

Note that an absorbing gas reduces the TOA radiance because light is lost to absorption. Correcting for this loss will increase the TOA radiance or reflectance, with the effect being greatest at blue wavelengths where multiple scattering is greatest.
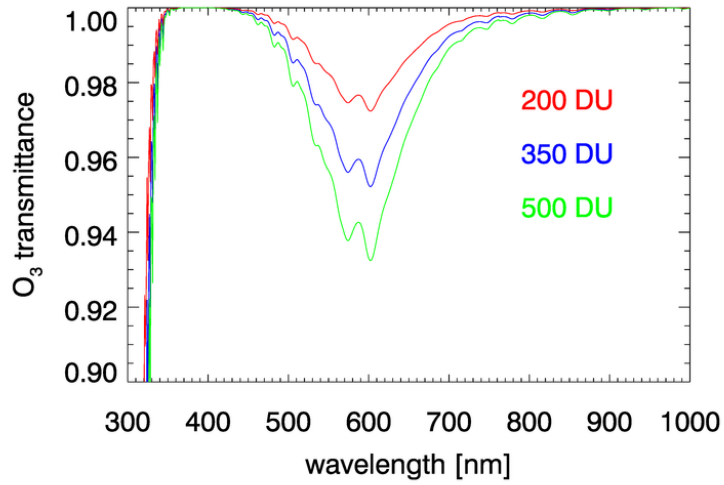
Figure 2: Transmittance by O_3 for 200, 350, and 500 Dobson units and a vertical path through the atmosphere.
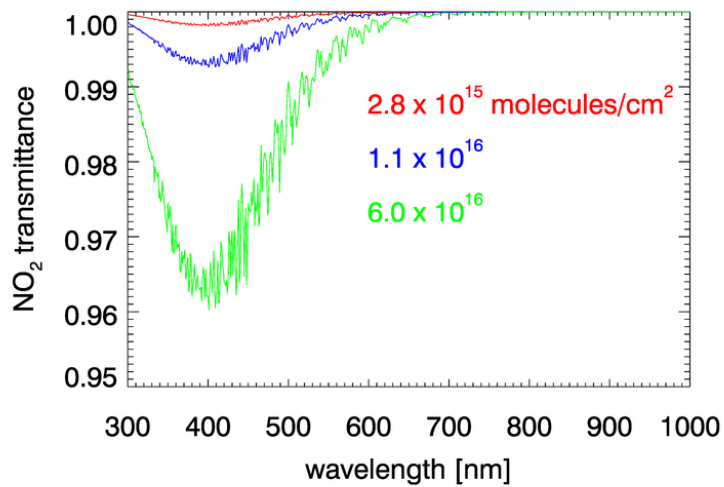

Figure 3: Transmittance by NO_2 for low (2.8×10^{15}), typical (1.1×10^{16}), and high (6.0×10^{16} molecules cm^{-2}) concentrations of NO_2 and a vertical path through the atmosphere.

Absorption by Ozone

The diffuse transmission by ozone can be written as

$$t_{O_3} = \& \exp\left[-\tau_{O_3}\left(\frac{1}{\cos\theta_s} + \frac{1}{\cos\theta_v}\right)\right] \tag{2}$$
$$= \& \exp\left[-\tau_{O_3}M\right],$$

where M is the geometric air mass factor defined in Eq. (equation1), and τ_{O_3} is the optical thickness of the ozone for a vertical path through the atmosphere. Scattering by ozone is negligible, but absorption is significant at some wavelengths. Thus τ_{O_3} is the optical thickness for absorption by ozone, which is given by

$$\tau_{O_3}(\lambda) = [O_3]k_{O_3}(\lambda), \tag{3}$$

where $[O_3]$ is the ozone concentration (column amount in molecules cm^{-2}), and k_{O_3} is the absorption cross section (in cm^2 molecule^{-1}). The ozone concentration $[O_3]$ for a given image pixel is obtained from the NASA OMI or TOMS sensors (Ozone Monitoring Instrument; Total Ozone Mapping Spectrometer, now replaced by OMI).

As was seen in for transmittance in Figs. figure2 and figure3, the absorption cross sections for gases like O_3 and, especially, NO_2 can vary with wavelength on a nanometer scale. To fully resolve the effects of such wavelength dependence on sensor signals, radiative transfer calculations would require computationally intensive "line-by-line" calculations followed by integration over the sensor bands. To avoid that computational expense, band-averaged values of the Rayleigh optical depth and absorption cross sections k_{O_3} and k_{NO_2} are computed for each sensor and tabulated. Radiative transfer calculations then use the band-averaged values with just one radiative transfer calculation done for each sensor band. These band-averaged values depend on the sensor even for the same nominal wavelength band (e.g, the 412 nm blue band) because of different band widths about the nominal center wavelength and different sensor response functions within a band. Figure figure4 shows example band-averaged values for the VIIRS and MODIS Aqua sensors.

Absorption by NO_2

Nitrogen dioxide NO_2 occurs both in the stratosphere and near the Earth's surface. NO_2 in the lower atmosphere is generated primarily by human activities (automobiles, industry, fires), and the highest concentrations are near the earth's surface in industrial areas. Numerical simulations show that failure to correct for absorption by NO_2 can give errors of approximately 1% in TOA radiances at blue wavelengths, which result in $\sim 10\%$ errors in retrieved water-leaving radiances (Ahmad et al. (2007)).

The geometric air mass factor M of Eq. (equation1) and a simple atmospheric transmittance function like that of Eq. likesection2) are valid for ozone absorption corrections because scattering by ozone in the upper atmosphere is negligible. However, such functions may be not adequate for NO_2 correction calculations because of multiple scattering in the dense lower atmosphere. Further guidance for the form of the NO_2 correction comes from
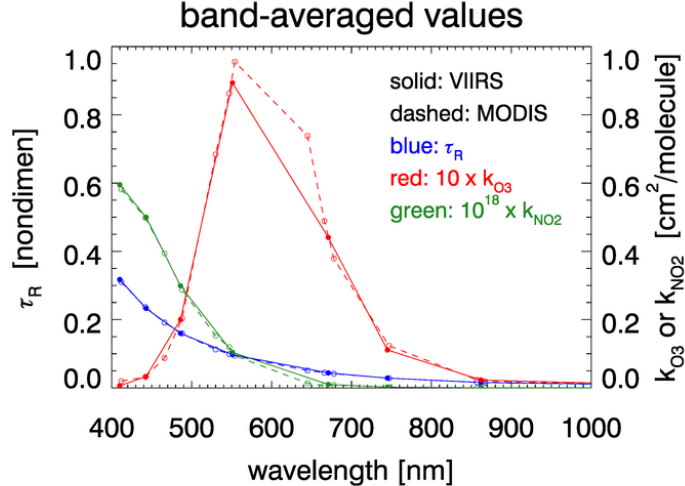
Figure 4: Band-averaged Rayleigh optical depth τ_R, ozone absorption cross section k_{O_3}, and NO_2 absorption cross section k_{NO_2} for the VIIRS and MODIS Aqua sensors. (Data from NASA ocean color documents)

the observation that the water-leaving radiance L_w sees all NO_2 in the atmosphere, so the total NO_2 concentration N must be used to correct L_w for NO_2 absorption. However, the upwelling atmospheric path radiance L_atm, which is generated throughout the atmosphere, is not strongly influenced by the absorbing gas very near the surface. Extremely accurate numerical simulations show that in that case, N', the NO_2 concentration between an altitude of 200 m and the TOA, can be used as a satisfactory measure of NO_2 concentration. This result leads to different corrections for the measured TOA path radiance and for the water-leaving radiance.

Let ρ_obs be the uncorrected, observed (measured) TOA reflectance, and let ρ_corr be the TOA reflectance corrected for NO_2 absorption effects. Comparison of numerical simulations and analytical approximations justifies a correction of the form

$$\rho_\mathrm{corr} = \rho_\mathrm{obs} \exp\left[\alpha N'\left(\frac{1}{\cos\theta_\mathrm{s}} + \frac{1}{\cos\theta_\mathrm{v}}\right)\right],$$

where N' is the NO_2 concentration between an altitude of 200 m and the TOA. This simple formula gives ρ_corr values that are within 0.15% of the values obtained by exact numerical simulations that account for the total column NO_2 concentration and multiple scattering.

The correction for water-leaving radiance proceeds as follows. The reflectances can be written as (Ahmad et al. (2007), Eqs. 1 and 7)

$$\rho_t(\theta_\mathrm{s}, \theta_\mathrm{v}) = \rho_\mathrm{path}(\theta_\mathrm{s}, \theta_\mathrm{v}) + t_3(\theta_\mathrm{v})t_d(\theta_\mathrm{s})\rho_\mathrm{w}(\theta_\mathrm{s}, \theta_\mathrm{v}) + \text{glint and whitecap terms}$$

(omitting the arguments for wavelength, azimuthal angle, and wind speed). Here t_3 is the diffuse transmission along the viewing direction from the sea surface to the sensor, t_d is the diffuse transmission of downwelling solar irradiance, and ρ_w is the water-leaving reflectance at the sea surface. Consider now only the path and water-leaving terms, and omit the directional

4

arguments for brevity. Then multiplying this equation by the exponential correction factor for the observed TOA reflectance gives

$$
\begin{aligned}
\rho_{\mathrm{t}} \exp\left[\alpha N'\left(\sec\theta_{\mathrm{s}} + \sec\theta_{\mathrm{v}}\right)\right] = {}& \& \rho_{\mathrm{path}} \exp\left[\alpha N'\left(\sec\theta_{\mathrm{s}} + \sec\theta_{\mathrm{v}}\right)\right] \\
& + \& \left[t_3 \exp(\alpha N' \sec\theta)\right]\left[t_{\mathrm{d}}\rho_{\mathrm{w}} \exp(\alpha N' \sec\theta_{\mathrm{s}})\right].
\end{aligned}
$$

Numerical simulations show that both the path reflectance and the diffuse transmission term $[t_3 \exp(\alpha N' \sec\theta)]$ are accurate to within 0.2% with this correction. However, the error in the water-leaving factor, $[t_{\mathrm{d}}\rho_{\mathrm{w}} \exp(\alpha N' \sec\theta_{\mathrm{s}})]$ is in error by 0.5 to 1.5%, which is unacceptably large. The reason for the greater error in this term is that it depends on the downwelling irradiance, which passes through the entire atmosphere and thus sees the total concentration N, not just the reduced concentration N' that is adequate for correction of the TOA path term. However, the error in this term also decreases to $\sim 0.2\%$ if N' is replaced by N. This error can be reduced still further by the following empirical procedure.

For bands where NO_2 absorption is significant (e.g., at 412 or 443 nm), the atmospheric correction is determined as always (without NO_2 correction) using the NIR bands. However, rather than subtract these terms from the corrected TOA reflectance, the atmospheric correction terms (including the Rayleigh reflectance) are reduced for NO_2 absorption by applying a factor of $\exp[-\alpha N'(\sec\theta_{\mathrm{s}} + \sec\theta_{\mathrm{v}})]$. The computed path reflectance for NO_2 is then subtracted from the observed TOA reflectance to obtain $\Delta\rho_{\mathrm{obs}} = t_3 t_d \rho_{\mathrm{w}}$, which is the TOA value for water-leaving reflectance in the presence of NO_2. The NO_2-corrected value of the water-leaving reflectance is then obtained by multiplying this $\Delta\rho_{\mathrm{obs}}$ by $\exp(\alpha N' \sec\theta) \exp(\alpha N \sec\theta_{\mathrm{s}})$, which gives

$$
\begin{aligned}
& \exp(\&\alpha N' \sec\theta) \exp(\alpha N \sec\theta_{\mathrm{s}})\Delta\rho_{\mathrm{obs}} \\
= {}& \& \left[t_3 \exp(\alpha N' \sec\theta)\right]\left[t_{\mathrm{d}}\rho_{\mathrm{w}} \exp(\alpha N \sec\theta_{\mathrm{s}})\right].
\end{aligned}
$$

Note that $t_3 \exp(\alpha N' \sec\theta)$ is the NO_2-corrected transmission term, and $\rho_{\mathrm{w}}' = t_{\mathrm{d}}\rho_{\mathrm{w}} \exp(\alpha N \sec\theta_{\mathrm{s}})$ is the desired NO_2-corrected water-leaving reflectance. This equation is then solved to obtain ρ_{w}':

$$
\rho_{\mathrm{w}}' = \frac{\exp(\alpha N' \sec\theta) \exp(\alpha N \sec\theta_{\mathrm{s}})\Delta\rho_{\mathrm{obs}}}{t_3 \exp(\alpha N' \sec\theta)} \, . \tag{4}
$$

Note that the exponentials are increasing the magnitude of the water-leaving radiance compared to the no-NO_2 case, which accounts for the loss due to NO_2 absorption along the paths of the Sun's direct beam and the viewing direction. The term for the Sun's direct beam uses the full column NO_2 concentration N, whereas the viewing-path term uses the reduced concentration N'. This is an artifice that brings the analytical correction of Eq. (likesection4) into close agreement with the exact numerical calculations. The absorption cross section α is a function of wavelength. Computations are done for α at 18 deg C, and then a temperature correction is made. (Ahmad's Table 1 gives the band-averaged NO_2 absorption cross sections for SeaWiFS and MODIS bands, which are called σ in that table. This σ is same quantity as α in his Eq. (4) and in the equations of this chapter.)